ResearchGate

See discussions, stats, and author profiles for this publication at:
https://www.researchgate.net/publication/222635999

A TDDFT study of the electronic spectrum of s-tetrazine in the gas-phase and in aqueous solution

ARTICLE *in* CHEMICAL PHYSICS LETTERS · NOVEMBER 2000

Impact Factor: 1.9 · DOI: 10.1016/S0009-2614(00)01082-4

CITATIONS
157

READS
48

2 AUTHORS, INCLUDING:

Vincenzo Barone
Scuola Normale Superiore di Pisa
774 PUBLICATIONS **44,771** CITATIONS

SEE PROFILE

Available from: Vincenzo Barone
Retrieved on: 26 January 2016

3 November 2000

ELSEVIER

Chemical Physics Letters 330 (2000) 152–160

CHEMICAL PHYSICS LETTERS

www.elsevier.nl/locate/cplett

A TDDFT study of the electronic spectrum of s-tetrazine in the gas-phase and in aqueous solution

Carlo Adamo, Vincenzo Barone *

Dipartimento di Chimica, Università 'Federico II', via Mezzocannone 4, I-80134 Napoli, Italy

Received 10 August 2000; in final form 19 September 2000

Abstract

Time-dependent density functional theory (TDDFT) is applied to calculate vertical excitation energies of s-tetrazine, both in the gas-phase and in aqueous solution. The model density functional (PBE0) is obtained by combining the Perdew–Burke–Erzenrhof (PBE) generalized gradient functional with a predetermined amount of exact exchange, while the polarizable continuum model (PCM) is used to mime solvent effects on electronic transitions. Our results in the gas-phase show that the PBE0 functional provides accurate excitations both to valence and to low-lying Rydberg states. At the same time, the experimental solvent shifts in aqueous solution are well reproduced when the solute and the first solvation shell are embedded by a continuum solvent. These results show the potentialities of the combined TDDFT/PCM approach for the study of UV spectra of aromatic compounds. © 2000 Elsevier Science B.V. All rights reserved.

1. Introduction

The prediction and interpretation of the discrete part of optical and ultraviolet (UV) spectra is an important goal in several chemical domains, but it remains a very demanding task for quantum mechanical methods, especially for medium- and large-sized molecules of chemical interest. Furthermore, solute–solvent interactions tune the shape and the intensities of the observed spectra and provide, through spectral line shifts, important interpretative aids in the band assignment. Thus, an inexpensive yet accurate method for calculating vertical excitation energies, both in vacuum and in solution, would be an invaluable tool.

Density functional theory (DFT) has been remarkably successful in providing means for an accurate evaluation of ground state properties [1]. On these grounds, interest is now shifting toward an accurate and physically sound extension of DFT to the study of excited electronic states. In this context, the time-dependent generalization of the DFT theory (TDDFT) appears especially promising since it couples formal rigor with effectiveness [2–5]. Several tests [6,7] have shown that implementation of last generation model functionals in a TDDFT framework provides remarkable results for low excitation energies. However, it has been claimed that reliable vertical excitation energies to Rydberg states can be computed only using more sophisticated tools, like, e.g., the so-called asymptotically corrected potentials [6,8]. We have recently found that the so-called PBE0 model [9], a hybrid Hartree–Fock (HF)/Kohn–Sham (KS) approach based on the

* Corresponding author. Fax: +39-81-552-7771.
E-mail address: enzo@lsdm.dichi.unina.it (V. Barone).

0009-2614/00/$ - see front matter © 2000 Elsevier Science B.V. All rights reserved.
PII: S0009-2614(00)01082-4

Perdew–Burke–Erzenrhof (PBE) exchange-correlation functional [10], provides vertical excitation energies in good agreement with experimental data [11,12]. Furthermore, this method handles with the same accuracy excitations to both valence and low-lying Rydberg states, even in the presence of non-negligible contributions from double excitations [12]. At the same time, PBE0 is a reliable tool for ground state properties, including geometries, frequencies and spectroscopic parameters [9,13]. The strength of this approach is, in our opinion, that the parent PBE functional does not contain any parameter fitted to experimental data and that a predefined amount of HF exchange is added self-consistently to the DFT contribution.

As mentioned above, solute–solvent interactions have a direct and significant influence on UV spectra, especially on $n \rightarrow \pi^*$ and Rydberg excitations. As a general rule, $n \rightarrow \pi^*$ transitions are significantly blue-shifted, whereas Rydberg excitations are only weakly red-shifted. As a consequence a reliable theoretical study of electronic spectra cannot be performed without a proper treatment of solute–solvent interactions. Effective Hamiltonian – continuum solvent models appear particularly attractive in this connection and have been recently extended to the study of non-equilibrium solvent effects, like those involved in electronic excitations [15–18].

S-tetrazine represents an interesting benchmark since the analysis of its spectrum requires a balanced treatment of $n \rightarrow \pi^*$, $\pi \rightarrow \pi^*$ and Rydberg excitations. Thus a number of quantum mechanical models have been applied to this system (see for instance Refs. [19–23] and compared with the rich and well-resolved experimental spectrum [24–27]. In particular, the results of a recent TDDFT study [22] showed an irregular behavior with respect to refined post-HF results, thus leading the authors to conclude that DFT studies of excitation spectra must be carried out with great care. These conclusions are in some contrast with our initial studies on aromatic systems, which showed how the PBE0/TDDFT approach is a valuable alternative to the more expensive post-HF methods [11]. This situation has prompted us to investigate the performances of the PBE0 functional in predicting the complete manifold of vertical excitations by the TDDFT approach, without any computational bias beyond the choice of the atomic basis set. At the same time we test our recent implementation of the TDDFT/PCM approach for computing solvent shifts of UV spectra in aqueous solution: while experimental results are available for the two lowest $n \rightarrow \pi^*$ transitions [25], we are not aware of any previous quantum mechanical computation.

2. Computational details

All the computations described in this work have been performed using a development version of the GAUSSIAN package [28] using the PBE [10] and PBE0 [9] functionals. The latter parameter-free hybrid model is based on previous work by Becke [29] and Perdew [30] and delivers reliable results for several physico-chemical properties including excitation energies [9,11–13]. The specific implementation of TDDFT used in the present study is described in detail in Ref. [7].

All the ground state molecular structures have been optimized with the 6-311G(d,p) basis set [31] since previous experience has showed that a polarized valence triple-ζ basis set generally provides nearly converged structural parameters by DFT methods [1]. Vertical excitation energies have been computed using both the 6-311++G(d,p) [31] and the augmented Sadlej [32,33] (referred to in the following as Sadlej+) basis sets, which should allow a good description of low-lying valence and Rydberg states [11,12,34].

Continuum solvent approaches have been described in detail in a number of Letters and reviews to which the reader is referred [14–18]. Here we just remember that in the so-called polarizable continuum model (PCM) the solute–solvent interactions are described in terms of a set of solvation charges spread on the surface of the cavity containing the solute. These charges are found by solving the linear system

$$\mathbf{Dq} = -\mathbf{b}, \tag{1}$$

where column vectors $\mathbf{q}$ and $\mathbf{b}$ collect the solvation charges and the solute electrostatic potentials computed at representative points of the cavity

surface and D matrix depends on the solvent dielectric constant and on cavity geometrical elements [14]. The CPCM variant used in the present work [16] employs conductor rather than dielectric boundary conditions and this leads to a simpler and more robust implementation. Several studies have shown that for polar solvents the results obtained by different versions of PCM are very close. Non-equilibrium solvent effects, like those occurring during electronic excitations, can be introduced by splitting solvation charges into two components [17,18]

$$q_i = q_{i,\mathrm{f}} + q_{i,s}, \tag{2}$$

where $q_{i,\mathrm{f}}$ is the charge due to the electronic (fast) component of solvent polarization, which follows the solute changes upon excitations, and $q_{i,s}$ is the charge from the orientational (slow) part, which is delayed when the solute undergoes a sudden transformation. Since the latter contribution has to be frozen during excitations, the solvation charges are found solving two systems of equations

$$\mathbf{D}(\varepsilon)\mathbf{q} = -\mathbf{b}, \tag{4a}$$

$$\mathbf{D}(\varepsilon_{\mathrm{f}})\mathbf{q}_{\mathrm{f}} = -(\mathbf{b} + \mathbf{b}_s). \tag{4b}$$

Eq. (4a) is simply Eq. (2) with the explicit indication of the dependence on the static dielectric constant (ε). In Eq. (4b), the fast dielectric constant, ε_{f}, is used instead and vector $\mathbf{b}_s$ collects the electrostatic potentials generated by the slow charges at the representative points of the cavity surface. Further details both of the formal derivation and of the numerical implementation can be found in Refs. [17,18].

3. Results and discussion

Before discussing our results, we recall some difficulties connected with the application of TDDFT. Several letters have shown that current functionals, including some HF/DFT hybrid approaches like B3LYP, underestimate the excitation energies of Rydberg states [8,11,34]. The origin of this problem has been traced back to the failure of approximate exchange-correlation functionals to correctly describe the potential in the asymptotic region [8]. One way out is represented by asymptotically correct potentials, like those proposed in Ref. [8] (HCTH(AC)). However, these potentials do not have an associated functional, so that total energies and energy derivatives (required for geometry optimization, frequencies and other properties) cannot be evaluated at the same level (with the same functional), thus introducing some unbalance in the computational protocol. In hybrid functionals, instead, the asymptotic potential comes closer to the correct behavior, since it decays as $-a/r$, where a is some constant other than 1 [6,22]. The reliability of the PBE0 model is further enhanced by the remarkably good behavior of the underlying PBE functional in low-density high-gradient regions which are particularly important for polarizabilities and excitation energies [9,11].

All the vertical electronic transitions have been computed at the geometry of the singlet ground electronic state. The molecule has D_{2h} symmetry and is oriented in the yz-plane with the CH bonds lying along the z-axis. The optimized PBE0/6-311G(d,p) bond lengths (CN = 1.331 Å, NN = 1.332 Å, CH = 1.085 Å) are close to their experimental (X-ray) counterparts (CN = 1.338 Å, NN = 1.326 Å, CH = 1.073 Å [35]). Test computations have shown that slightly different geometrical parameters (e.g., those used for CASPT2 computations in Ref. [23]) lead to very similar excitation energies. The excitations of s-tetrazine computed by the TDDFT approach using both the PBE and the PBE0 functionals are compared in Table 1 with the available experimental results. The most striking feature of these data concerns the 2^1A_g and 1^1B_{3g} excited states, which do not appear in the PBE0 spectrum. These two states arise from $n \rightarrow \pi^*$ transitions, with a double excitation character, which cannot be reproduced by first-order TDDFT methods [22].

Excluding these excitations, which are not experimentally detected, there is a good agreement between the PBE0 results and the available experimental data. In fact the mean average error (m.a.e), computed with respect to the 11 observed transitions (see Table 1), is 0.26 eV at the PBE0/6-311+G(d,p) level.

In Table 2 are reported also the results of the most reliable general post-HF approaches to excited states, namely CASPT2 and Ext-STEOM-

Table 1
Computed excitation energies (eV) for the singlet excited states of s-tetrazine[a]

Symmetry	Transition	Character	exp[b]	CAS-PT2[c] ANO	Ext-STE OM-CC[d] Sadlej+	HCTH(AC)[e] Sadlej+	PBE 6-311++ G(d,p)	PBE0 6-311++G(d,p)	PBE0 Sadlej+
$1B_{3u}$	$n \rightarrow \pi^*$	$3b_{3g} \rightarrow 1a_u$	2.25	1.96	2.22	1.90	1.78	2.23	2.25
$1A_u$	$n \rightarrow \pi^*$	$3b_{3g} \rightarrow 2b_{3u}$	3.4	3.06	3.62	2.90	2.68	3.45	3.47
$2A_g$	$nn \rightarrow \pi^*\pi^*$	$3b_{3g}^2 \rightarrow 1a_u^2$		4.37	5.06	No	No	No	No
$1B_{1g}$	$n \rightarrow \pi^*$	$5b_{1u} \rightarrow 1a_u$		4.51	4.73	4.23	4.10	4.86	4.85
$1B_{2u}$	$\pi \rightarrow \pi^*$	$1b_{2g} \rightarrow 1a_u$	4.97	4.89	4.90	5.54	5.65	5.83	5.81
$1B_{2g}$	$n \rightarrow \pi^*$	$4b_{2u} \rightarrow 1a_u$		5.05	5.09	4.97	4.92	5.66	5.67
$1B_{3g}$	$nn \rightarrow \pi^*\pi^*$	$3b_{3g}^2 \rightarrow 1a_u 2b_{3u}$		5.16	6.30	No	No	No	No
$2A_u$	$n \rightarrow \pi^*$	$6a_g \rightarrow 1a_u$	5.0	5.28	5.23	4.82	4.74	5.32	5.34
$2B_{2g}$	$n \rightarrow \pi^*$	$5b_{1u} \rightarrow 2b_{3u}$		5.48	6.16	5.33	5.20	6.08	6.07
$2B_{1g}$	$n \rightarrow \pi$	$4b_{2u} \rightarrow 2b_{3u}$ $3b_{3g} \rightarrow 2b_{2g}$		5.99	7.06	6.04	5.99	7.65	7.61
$2B_{3g}$	Ry	$3b_{3g} \rightarrow 7a_g$	5.92	6.02	6.47	6.00	5.32	6.34	6.23
$2B_{3u}$	$n \rightarrow \pi^*$	$6a_g \rightarrow 2b_{3u}$	6.34	6.37	6.53	5.84	5.68	6.50	6.50
$3B_{1g}$	$n \rightarrow \pi^*$	$4b_{2u} \rightarrow 2b_{3u}$		6.20	6.73	6.65	6.51	6.99	6.95
$2B_{2u}$	Ry	$3b_{3g} \rightarrow 6b_{1u}$	7.19	6.75	7.29	6.70	5.72	6.84	6.77
$3A_u$	Ry	$3b_{3g} \rightarrow 3b_{3u}$		6.80	7.62	6.84	6.67	7.67	7.35
$2B_{1u}$	Ry	$3b_{3g} \rightarrow 5b_{2u}$	7.6	6.96	7.99	7.19	6.75	7.99	7.86
$3B_{1u}$	$\pi \rightarrow \pi^*$	$1b_{1g} \rightarrow 1a_u$	7.1	7.13	7.14	6.84	7.05	7.11	7.06
$3B_{3g}$	Ry	$3b_{3g} \rightarrow 8a_g$		7.36	7.78	7.15	6.49	7.51	7.44
$5B_{1u}$	$\pi \rightarrow \pi^*$	$1b_{2g} \rightarrow 2b_{3u}$	7.6	7.54	7.64	7.51	7.59	7.73	7.57
$4B_{1g}$	Ry	$3b_{3g} \rightarrow 2b_{2g}$		7.55	8.07	7.65	7.65	8.75	8.44
$4A_g$	Ry	$3b_{3g} \rightarrow 4b_{3g}$		7.62	8.11	7.56	7.03	8.07	7.86
$4B_{3g}$	Ry	$3b_{3g} \rightarrow 3b_{2g}$		7.72	7.81	7.71	8.46	9.42	8.51
$3B_{2g}$	Ry	$5b_{1u} \rightarrow 2b_{3u}$		7.77	8.06	7.75	8.59	8.97	8.81
$4B_{2u}$	$\pi \rightarrow \pi^*$	$1b_{1g} \rightarrow 2b_{3u}$	8.3	7.94	8.28	8.19	8.17	8.56	8.50

[a] The PBE0 values have been computed at the PBE0/6-311G(d,p) geometry of the ground electronic state.
[b] Ref. [27].
[c] Ref. [21].
[d] Ref. [23].
[e] Ref. [22].

Table 2
Computed excitation energies (eV) for the triplet excited states of s-tetrazine[a]

Symmetry	Transition	Character	exp[b]	CAS-PT2[c] ANO	Ext-STEOM-CC[d] Sadlej	PBE0 6-311++G(d,p)	PBE0 Sadlej+
$1\ B_{3u}$	$n \rightarrow \pi^*$	$3b_{3g} \rightarrow 1a_u$	1.69	1.45	1.71	1.35	1.38
$1A_u$	$n \rightarrow \pi^*$	$3b_{3g} \rightarrow 2b_{3u}$	2.9	2.81	3.47	3.01	3.03
$1B_{1g}$	$n \rightarrow \pi^*$	$5b_{1u} \rightarrow 1a_u$	3.6	3.76	3.97	3.68	3.69
$1B_{1u}$	$\pi \rightarrow \pi^*$	$1b_{1g} \rightarrow 1a_u$		4.25	3.67	3.92	3.91
$1B_{2u}$	$\pi \rightarrow \pi^*$	$1b_{2g} \rightarrow 1a_u$	4.2	4.29	4.35	4.22	4.17
$1B_{2g}$	$n \rightarrow \pi^*$	$4b_{2u} \rightarrow 1a_u$		4.67	4.78	4.67	4.74
$2A_u$	$n \rightarrow \pi^*$	$6a_g \rightarrow 1a_u$	4.6	4.85	4.89	4.72	4.68
$1B_{3g}$	$\pi \rightarrow \pi^*$	$3b_{3g} \rightarrow 7a_g$		5.08	6.48	6.29	6.18
$2B_{1u}$	$\pi \rightarrow \pi^*$	$1b_{1g} \rightarrow 1a_u$	5.2	5.09	5.31	5.41	5.37
$2B_{2g}$	$n \rightarrow \pi^*$	$5b_{1u} \rightarrow 2b_{3u}$		5.30	6.16	5.76	5.75
$2B_{1g}$	$n \rightarrow \pi^*$	$4b_{2u} \rightarrow 2b_{3u}$		5.68	6.77	6.61	6.61
$2B_{3u}$	$n \rightarrow \pi^*$	$6a_g \rightarrow 2b_{3u}$	6.4	6.14	6.54	6.13	6.14
$2B_{2u}$	$\pi \rightarrow \pi^*$	$1b_{1g} \rightarrow 2b_{3u}$	6.9	6.81	7.36	6.80	6.73

[a] The PBE0 values have been computed at the PBE0/6-311G(d,p) geometry of the singlet state.
[b] Ref. [27].
[c] Ref. [21].
[d] Ref. [23].

CC. We point out that, despite their accuracy, multi-reference method, like CASPT2, require a careful choice of computational parameters (e.g., active space and/or level shifting), whereas single reference methods based on the coupled cluster (CC) approach like the equation of motion CC (EOM-CC) method, come close to the so-called 'black box' methods which do not involve any arbitrary decision by the user. EOM-CC methods are reliable in the prediction of vertical excitation energies for states dominated by single excitations and have been recently extended to include doubly excited states (Ext-STEOM-CC) [23]: unfortunately the scaling of these methods with the number of electrons makes their use prohibitive for large chemically significant systems.

The m.a.es of PBE0 (0.26 eV) and CASPT2 (0.24 eV) are very close and only slightly larger than that of Ext-STEOM-CC (0.18 eV). The largest discrepancy is found for the 1^1B_{2u} transition, which falls at 5.81 eV at the PBE0 level, 0.8 eV higher than the experimental finding [27]. The other $\pi \rightarrow \pi^*$ excitations are reproduced with a better precision, with all the DFT (conventional or hybrid) approaches providing comparable deviations from the experimental values (between 0.6 and 0.7 eV).

As concerns the other transitions, not detected experimentally, we consider in the following Ext-STEOM-CC computations as references. The PBE0 and Ext-STEOM-CC results are in good agreement for these transitions, irrespective of their nature ($\pi \rightarrow \pi^*$, $n \rightarrow \pi^*$, and Rydberg), with differences ranging between 0.1 (2^1B_{1g}) and 0.4 (3^1B_{3g}) eV.

Some general trends are apparent in our results. The $\pi \rightarrow \pi^*$ transitions are described well already by conventional DFT approaches (like PBE) and inclusion of some HF exchange does not lead to large variations (max 0.3 eV). In contrast, Rydberg states are better reproduced by functionals including some HF exchange. This behavior is evident by a detailed analysis of the data in Table 1. The PBE and PBE0 results for the $n \rightarrow \pi^*$ and Rydberg transitions are significantly different, whereas PBE0 and HCTH(AC) values are close to each other. Anyway, a deterioration in the reproduction of the highest Rydberg states is found at the PBE0 level due to the collapse of vertical excitations at energies higher than the ionization threshold (−7.3 eV at the PBE0/6-311+G(d,p) level). This effect is well known for the TDDFT methods [6,11], and hybrid functionals, introducing a fraction of exact exchange only shifts the problem toward higher transitions [11,34].

More subtle effects rule, instead, $n \rightarrow \pi^*$ excitations. Here an increase of transition energies,

between 0.5 and 0.8 eV, is found going from PBE to PBE0. In a simple ΔSCF scheme, the origin of this behavior can be ascribed to the variation of the orbital energies on inclusion of some HF exchange. In fact, the n occupied orbitals are stabilized by the inclusion of the HF exchange, while the π^* orbitals are destabilized. The net effect is an increase of the orbital energy gaps in PBE0 w.r.t. PBE. The different character of the orbitals involved in the lowest $n \rightarrow \pi^*$ excitations is clear from Fig. 1, where the highest n orbitals ($3b_{3g}$, n, and $1b_{2g}, \pi$) as well as the lowest π^* orbitals ($1a_u$, LUMO, and $2b_{3u}$) are plotted.

Finally, extension of the basis set does not determine any significant variation in the computed $\pi \rightarrow \pi^*$ and $n \rightarrow \pi^*$ transitions. In contrast, Rydberg states higher than 8 eV are significantly stabilized in going from the 6-311++G(d,p) to the Sadlej basis set. In particular, the largest effect is found for the 4^1B_{3g} state, whose energy drops from 9.42 to 8.51 eV.

Table 2 collects the excitation energies computed for triplet states. For comparison purpose, the values obtained in the Ext-STEOM-CC and CASPT2 studies [21,23] are reported, together with the data obtained from electron energy loss (EEL) experiments [26]. Once again an overall good agreement is found between the computed PBE0 transitions and the experimental findings. As a matter of fact, the m.a.es of PBE0 (0.16 eV) and CASPT2 (0.15 eV) results are comparable, but they are now significantly lower than those of Ext-

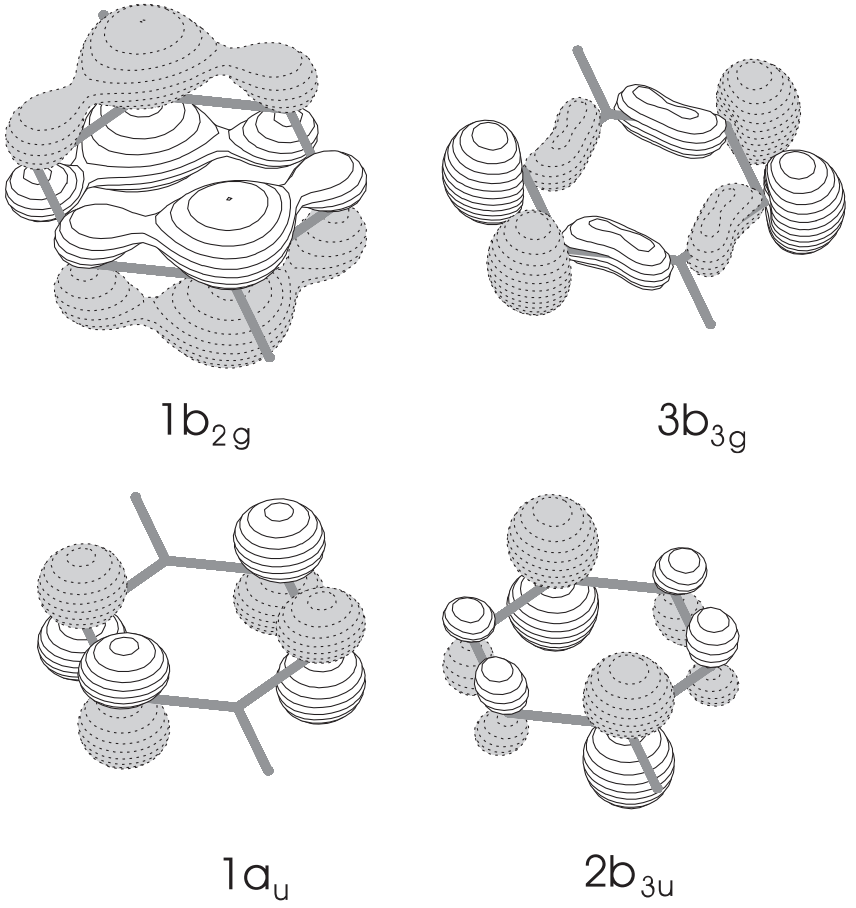

Fig. 1. Plots of the most important orbitals involved in the vertical excitations of s-tetrazine.

STEOM-CC computations (0.25 eV). Interestingly, the PBE0 calculations reproduce well the energy of the second triplet state (1^3A_u), which significantly overshoots at the CC level [23]. Some other important discrepancies are found between the different quantum mechanical models for the vertical transitions which are not observed experimentally. The most striking difference concerns the 1^3B_{3g} state, which is 6.3 eV higher than the singlet state at the PBE0 level, in agreement with CC computations, while the CASPT2 results is 5.1 eV [21]. Other significant differences are found for the excitations to the $b_{3u}(\pi^*)$ orbitals. Finally, we note that the 1^3B_{1u} and the 1^3B_{2u} states are nearly degenerate at the CASPT2 level, a characteristic not found in our computations and in the CC study [21].

As mentioned in the introduction the UV spectrum of s-tetrazine has been recorded also in aqueous solution [25], and considerable blue-shifts are observed for the lowest $n \rightarrow \pi^*$ transitions. In particular, the 1^1B_{3u} transition increases from 2.3 eV in the gas-phase to 2.4 eV in aqueous solution, while a larger shift is found for the 1^1A_u band (+0.7 eV). Table 2 collects the TDDFT results in solution obtained using the PBE0/CPCM approach. In qualitative agreement with the experimental data, our results indicate that both the lowest $n \rightarrow \pi^*$ transitions are blue-shifted, the effect being larger for the 1^1A_u (0.2 eV) than for the $^1B_{3u}$ (0.1 eV) state. Solvent influences to a lower extent the higher $n \rightarrow \pi^*$ transitions, which are blue-shifted by about 0.2 eV. The $^1B_{2u}$ state is correctly red-shifted by our model, being originated by a π–π^* transition.

The quantitative difference in the solvent shifts of the two lowest $n \rightarrow \pi^*$ transitions arises from the different nature of the virtual orbitals involved, since both excitations are generated from the HOMO (see Table 1). As a matter of fact, the π^* orbital involved in the lowest transition (^1a_u), is strongly concentrated on nitrogen atoms, thus being easily polarized (and stabilized) by the solvent; this effect is not present in the π^* orbital involved in the second transition ($^2b_{3u}$), which is essentially concentrated on carbon atoms (see Fig. 1). As a consequence, the solvatochromic shift for the ^1A_u excitation is larger than for the $^1B_{3u}$ transition, in agreement with the experimental evidence.

Despite the qualitatively correct results, the solvent shift of the ^1A_u excitation is strongly underestimated. To better investigate this point, we reoptimized the geometry of s-tetrazine in aqueous solution by means of CPCM/PBE0/6-311G(d,p) computations. In the present case even a polar solvent like water, does not induce significant variations in the geometrical parameters, all the bond lengths (1.331, 1.325 and 1.084 Å, for CN, NN and CH bonds, respectively) being close to those found in the gas-phase. As a consequence, relaxation of the geometry in solution does not introduce any significant variation in the computed vertical transitions. We have next analyzed possible limitations of the continuum model in describing solvent shifts. In the present context, the main problem is that in aqueous solution the lone-pair electrons of the nitrogen atoms are engaged in intermolecular hydrogen bonds, and the promotion of one of these electrons to a π orbital weakens hydrogen bonds. So, the water molecules involved in the first solvent shell, and strongly bonded to the s-tetrazine, are expected to have an influence on the UV spectrum in solution. To better underline this point, we have added in our PBE0 computations four explicit water molecules bonded to the nitrogen atoms of s-tetrazine. The resulting super-molecule is depicted in Fig. 2. The geometry of the whole cluster has been fully optimized at the PBE0/6-311G(d,p) level, with the only constraint of D_{2h} symmetry. Small variations in geometrical parameters have been found, the bond lengths being 1.330, 1.320 and 1.084 Å for CN, NN and CH bonds, respectively. The water molecules are strongly bonded to s-tetrazine, the dissociation energy being 6.8 kcal/mol for each molecule at the PBE0/6-311++G(d,p) level (including BSSE corrections). Since a lower energy is required to dissociate the water dimer (4.8 kcal/mol at the same computational level), we can reasonably suppose that the cluster of s-tetrazine with four water molecules has a significant lifetime in aqueous solution.

The five lowest vertical transitions for the cluster of s-tetrazine with four water molecules are reported in Table 3. The two lowest transitions are

Table 3
Computed excitations energies (eV) for the singlet excited states of s-tetrazine in gas-phase and in aqueous solution[a]

Symmetry	Transition	Exp[b]		PBE0 vacuum	PBE0 CPCM	PBE0 $4H_2O$	PBE0 $4H_2O$ + CPCM
		Gas-phase	Water				
$^1B_{3u}$	$n \rightarrow \pi^*$	2.25	2.43	2.25	2.34 (2.30)	2.35	2.45
^1A_u	$n \rightarrow \pi^*$	3.4	4.06	3.47	3.71 (3.64)	3.63	3.85
$^1B_{1g}$	$n \rightarrow \pi^*$			4.85	4.94 (4.93)	4.97	5.04
$^1B_{2u}$	$\pi \rightarrow \pi^*$			5.81	5.72 (5.74)	5.79	5.71
$^1B_{2g}$	$n \rightarrow \pi^*$			5.67	5.77 (5.76)	5.74	6.07

[a] The PBE0 values have been computed using the Sadlej basis set and the PBE0/6-311G(d,p) geometry of the ground electronic state in the gas-phase. In parenthesis are reported the transitions obtained using the geometry optimized in aqueous.
[b] Ref. [25].

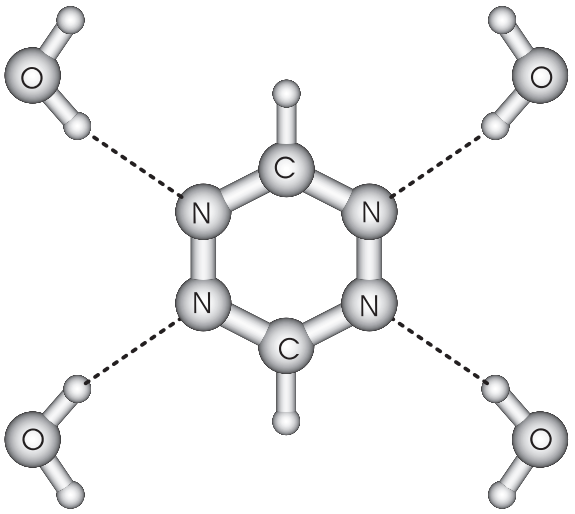

Fig. 2. Sketch of the cluster of s-tetrazine with four water molecules.

red-shifted by almost the same quantity found using the CPCM model: the $^1B_{3u}$ state is predicted at 2.4 eV, while the ^1A_u band is at 3.7 eV. As mentioned above, the nature of the two shifts is a direct consequence of the hydrogen bonding with the water molecules. Only the extent of shift is different for the two transitions, since the a_u orbital having a larger contribution from nitrogen atoms, is stabilized by the H-bonds.

The solvent effects found on the electronic spectrum of s-tetrazine with the continuum model and in the cluster are quantitatively similar, but different in nature. As a consequence they can act in a cooperative way: a further blue-shift of the $^1B_{3u}$ and ^1A_u transitions is observed embedding the cluster in a continuum solvent (last column of Table 3). It is noteworthy that at this level the lowest transition is reproduced quantitatively, while the ^1A_u excitation is only 0.2 eV lower than the experimental value [27].

4. Conclusion

In the present Letter, we have explored the behavior of the PBE0 functional in the evaluation of vertical excitation energies of s-tetrazine, both in the gas-phase and in aqueous solution. The results

obtained for a number of excitations, both to valence and to Rydberg states, are in good agreement with the available experimental data and with the results of the most-refined post-HF models. Next we have shown that an accurate description of the band shifts observed in solution can be obtained using a discrete/continuum solvent model. These results together with those already obtained for a wide class of chemical systems and properties [9,12,14] point out the advantages of using the same method (and almost the same basis set) for obtaining the different molecular features, ranging from geometries to thermochemical data and to vertical excitation energies.

References

[1] C. Adamo, A. di Matteo, V. Barone, Adv. Quantum Chem. 36 (1999) 45.
[2] E. Runge, E.K.U. Gross, Phys. Rev. Lett. 52 (1984) 997.
[3] M.E. Casida, in: D.P. Chong (Ed.), Recent Advances in Density Functional Methods, Part I, World Scientific, Singapore, 1995.
[4] M. Petersilka, U.J. Gossmann, E.K.U. Gross, Phys. Rev. Lett. 76 (1996) 1212.
[5] R. Bauernschmitt, R. Ahlrichs, Chem. Phys. Lett. 256 (1996) 454.
[6] M.K. Casida, C. Jamorski, K.C. Casida, D.R. Salahub, J. Chem. Phys. 108 (1998) 4439.
[7] R.E. Stratmann, G.E. Scuseria, M.J. Frisch, J. Chem. Phys. 109 (1998) 8128.
[8] D.J. Tozer, N.C. Handy, J. Chem. Phys. 109 (1998) 10180.
[9] C. Adamo, V. Barone, J. Chem. Phys. 110 (1999) 6158.
[10] J.P. Perdew, K. Burke, M. Ernzerhof, Phys. Rev. Lett. 77 (1996) 3865.
[11] C. Adamo, G.E. Scuseria, V. Barone, J. Chem. Phys. 111 (1999) 2889.
[12] C. Adamo, V. Barone, Chem. Phys. Lett. 314 (1999) 152.
[13] C. Adamo, M. Cossi, V. Barone, J. Mol. Struct. (Theochem.) 493 (1999) 145.
[14] J. Tomasi, M. Persico, Chem. Rev. 94 (1994) 2027.
[15] A. Klamt, J. Phys. Chem. 100 (1996) 3349.
[16] M. Cossi, V. Barone, J. Phys. Chem. A 102 (1998) 1995.
[17] M. Cossi, V. Barone, J. Chem. Phys. 112 (2000) 2427.
[18] M. Cossi, V. Barone, J. Phys. Chem. A, in press.
[19] H. Agren, S. Knuts, K. Mikkelsen, H.J.Aa. Jensen, Chem. Phys. 159 (1992) 211.
[20] J.E. Del Bene, J.D. Watts, R.J. Bartlett, J. Chem. Phys. 106 (1997) 6051.
[21] M. Rubio, B.O. Roos, Mol. Phys. 96 (1999) 603.
[22] D.J. Tozer, R.D. Amos, N.C. Handy, B.O. Roos, L. Serrano-Andres, Mol. Phys. 97 (1999) 859.
[23] M. Nooijen, J. Phys. Chem. A 104 (2000) 4553.
[24] R.C. Hirt, F. Halverson, R.G. Schmitt, J. Chem. Phys. 22 (1954) 1148.
[25] S.F. Mason, J. Chem. Phys. 29 (1959) 1263.
[26] A. Bolinos, P. Tsekeris, J. Philis, E. Pantos, G. Andritsopoulos, J. Mol. Struct. 102 (1984) 240.
[27] M.H. Palmer, N. McNab, D. Reed, A. Pollacchi, I. Walker, M.F. Guest, M.R.F. Siggel, Chem. Phys. 214 (1997) 191.
[28] M.J. Frisch et al., GAUSSIAN99 (Revision B.5), Gaussian Inc., Pittsburgh, PA, 1999.
[29] A.D. Becke, J. Chem. Phys. 104 (1996) 1040.
[30] J.P. Perdew, M. Ernzerhof, K. Burke, J. Chem. Phys. 105 (1996) 9982.
[31] R. Krishnan, J.S. Binkley, R. Seeger, J.A. Pople, J. Chem. Phys. 72 (1980) 650.
[32] A.J. Sadlej, Theor. Chim. Acta 79 (1993) 123.
[33] M.K. Casida, C. Jamorski, K.C. Casida, D.R. Salahub, J. Chem. Phys. 108 (1998) 4439.
[34] K.B. Wiberg, R.E. Stratmann, M.J. Frisch, Chem. Phys. Lett. 297 (1998) 60.
[35] K.K. Innes, I.G. Ross, W.R. Moomaw, J. Mol. Spectr. 132 (1988) 492.